Conception, numerical prediction and optimization of geomechanical measurements related to a vertical Mine-by-Test at the Meuse/Haute-Marne URL

Vincent Renaud, Franz Lahaie, Gilles Armand, Thierry Verdel, Pascal Bigarre

HAL Id: ineris-00174700

https://ineris.hal.science/ineris-00174700

Submitted on 25 Sep 2007

Conception, numerical prediction and optimization of geomechanical measurements related to a vertical Mine-by-Test at the Meuse/Haute-Marne URL

V. Renaud[a,*], F. Lahaie[a], G. Armand[b], T. Verdel[c], P. Bigarré[a]

[a] INERIS, Ecole de Mines de Nancy, 54042 Nancy Cedex, France

[b] Andra, Laboratoire souterrain de recherches Meuse/Haute-Marne, BP 9, 55290 Bure, France

[c] LaEGO, Ecole de Mines de Nancy, 54042 Nancy Cedex, France

ABSTRACT

Andra is conducting scientific experiments in the Meuse/Haute-Marne Underground Laboratory among which REP experiment is a vertical mine-by-test focusing on short and long term hydromechanical response of the argilite to the main shaft sinking. Displacements, strains, and pore pressures will be monitored while the shaft is passing down. Andra and INERIS intend to back-analyse most recorded geomechanical data based on under-excavation numerical technique in order to estimate pre-existing field stresses. The under-excavation interpretative technique consists in determining the pre-existing stress tensor related to a quite large volume of rock based on generalized inversion of geomechanical measurements recorded during the disturbance of the host rock (typically the excavation of an underground opening). In the framework a numerical study aiming to test accurately the sensitivity and numerical stability of this interpretative technique, 3D modelling of a step-by-step vertical mine-by-test, based on REP design, has been undertaken. One major step of the numerical

* Corresponding author. INERIS, Ecole de Mines de Nancy, 54042 Nancy Cedex, France. Tel.: +33(0)3 83 58 42 89; fax: +33(0)3 83 53 38 49.
E-mail address: vincent.renaud@ineris.fr.

procedure is to calculate each instrument response, coming up with a transient predicted measurement curve versus the progress of the shaft sinking. These important, intermediate results, on which this paper focuses, led the authors to several preliminary operational recommendations, e.g. relocation of sensors, which could not have been determined otherwise. These predictive numerical responses are of importance when a fast but efficient validation of the real data coming out from the field must be performed.

More generally, the authors intend to show how a synthetic, 3D numerical conception of a under-excavation interpretative experiment reveals to be unique method to explore different instrumentation layouts and optimize numerous options offered to the engineer in charge of its final design

Keywords: instrumentation, conception, design, under-excavation technique, numerical modelling, field stresses, measurement.

1. INTRODUCTION

1.1 OBJECT/CONTEXT

This study is part of the research related to REP experiment in the underground laboratory of Meuse/Haute-Marne (located at Bure, France).

Main objective of REP experiment is to study the short and long-term response of argillite to the sinking a vertical shaft (REP). The experiment will allow to record a great number of geomechanical measurements (strains, displacements, tilts.) around the excavated works. It is then possible to estimate, through a generalized numerical inversion, the pre existing stress field in the virgin rock mass.

Background literature and field experimentations show both this technique, known as the "under-excavation" or "undercoring" technique, as very promising.

The under-excavation technique was first described and proposed by Wiles and Kaiser [14, 15], which applied it quite successfully in the granitic context of the underground laboratory of the AECL (Atomic Energy off Canada Ltd, [10, 12, 13]). This technique was evaluated by Andra and INERIS in a marl formation (potash mining in Alsace: MDPA, France [3]) and clays type (Mont Terri, [4, 9]). These experiments allowed to confirm both all the interest of this technique [5] (even if it is not yet largely used [8]) while raising up some issues concerning its sensitivity and stability as regards both uncertainties affecting the important amount of input data handled and moreover the model used.

Research has then been undertaken based on numerical simulation of a standard, synthetic 3D experiment, aiming to a careful, detailed evaluation of this technique.
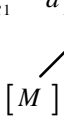
1.2 DESCRIPTION OF THE UNDER-EXCAVATION TECHNIQUE

The under-excavation technique requires several assumptions, whose principal one is the linear elastic behaviour of the rock mass. If several types of instruments are to be set up around the work (CSIRO cells, extensometers, inclinometers, convergence meters, clinometers, etc. figure 1), a linear relationship between strains/displacements and stresses can be expressed in the following matrix form: $\Delta \left\{ \begin{array}{c} \varepsilon \\ ... \end{array} \right\} = [M] \sigma$ (this implies an elastic behaviour).

[M] is the influence matrix.

$$
\begin{array}{l}
\text{strain (CSIRO sensors)} \\
\text{N measurements}
\end{array}\left.\right\}
\begin{bmatrix}
\Delta\varepsilon_1 \\
\vdots \\
\Delta\varepsilon_N \\
\Delta\lambda_1 \\
\vdots \\
\Delta\lambda_P \\
\Delta\gamma_1 \\
\vdots \\
\Delta\gamma_Q \\
\Delta\alpha_1 \\
\vdots \\
\Delta\alpha_Q
\end{bmatrix}
=
\begin{bmatrix}
a_{11} & a_{12} & a_{13} & a_{14} & a_{15} & a_{16} \\
\vdots & \vdots & \vdots & \vdots & \vdots & \vdots \\
a_{N1} & a_{N2} & a_{N3} & a_{N4} & a_{N5} & a_{N6} \\
b_{11} & b_{12} & b_{13} & b_{14} & b_{15} & b_{16} \\
\vdots & \vdots & \vdots & \vdots & \vdots & \vdots \\
b_{P1} & b_{P2} & b_{P3} & b_{P4} & b_{P5} & b_{P6} \\
c_{11} & c_{12} & c_{13} & c_{14} & c_{15} & c_{16} \\
\vdots & \vdots & \vdots & \vdots & \vdots & \vdots \\
c_{Q1} & c_{Q2} & c_{Q3} & c_{Q4} & c_{Q5} & c_{Q6} \\
d_{11} & d_{12} & d_{13} & d_{14} & d_{15} & d_{16} \\
\vdots & \vdots & \vdots & \vdots & \vdots & \vdots \\
d_{R1} & d_{R2} & d_{R3} & d_{R4} & d_{R5} & d_{R6}
\end{bmatrix}
\cdot
\begin{bmatrix}
\sigma_X^0 \\
\sigma_Y^0 \\
\sigma_Z^0 \\
\sigma_{YZ}^0 \\
\sigma_{XZ}^0 \\
\sigma_{XY}^0
\end{bmatrix}
\quad (1)
$$

$[M]$

where: $[\sigma^0]$ is the initial stress tensor and the a_{ij}, b_{ij} and c_{ij} are the influence coefficients respectively connecting the measurement variations of the sensors, with the components of the initial stress tensor $[\sigma^0]$ on the assumption of a linear elastic behaviour of the rock mass.

Determining the six components of the initial stress tensor amount thus to solve the system of $N+P+Q+\dots$ linear equations with 6 unknown. The difficulty of the under-excavation method lies in the direct problem: i.e. the determination of the coefficients of the matrix [M] which requires the numerical modelling of the experiment with 6 canonical loading schemes.

For each one of these 6 simulations and with each stage of work excavation, the method consists in recovering, at the location of each virtual sensor, the local value of the stress shift (for CSIRO cells), the new position (for extensometers and inclinometers), the new angle (clinometer), i.e. all induced perturbations due to the mining work progress. These values are then transformed into virtual measurements of strain (CSIRO cells), relative displacement (extensometer) and so on.

1.3 GENERAL CONSIDERATIONS

The synthetic experiment run consisted on the "virtual" monitoring of the progressive excavation of a 6.25 m in diameter vertical shaft around which were laid out beforehand different sensors,. Simulations have been carried out starting from the computer code FLAC^{3D} (transverse isotropic elastic behaviour + continuous and homogeneous medium).

3D mesh has been designed in order to fit as much as possible location of sensors, made in this case of 3 CSIRO cells, 3 multipoint extensometers and 1 multipoint inclinometer.

An additional calculation was carried out using results of triaxial loading tests in accordance with the one already estimated on the field. This was needed in order to check numerically several supplementary functionalities implemented in SYTGEOmath® interpretative tool developed by INERIS.

2. DESCRIPTION OF THE NUMERICAL MODEL

2.1 MODEL GEOMETRY

The model geometry is presented on figure 1. Dimensions of the model are 75 m x 75 m x 95 m: the lower and higher dimensions being respectively –515 m and –420 m. A meshing made up of 114009 elements, that is to say 120870 nodes was generated.

The model is defined in the coordinates system of principal stresses (X, Y, Z), which corresponds to a rotation of 25° of the general East-North (x, y, z) coordinates system. The meshing has been adapted to take into account the theoretical location of some measurement points (figure 1).

2.2 MECHANICAL PROPERTIES – EXCAVATION PROCESS

Input mechanical properties data are those presented in chapter VI of Andra report "Geological Referential of the site of East" [1]. They are summarized for each main geological facies in table 1. The shear modulus G_{13} of the transverse isotropic elastic law was calculated with the relation of Lekhnitskii [7], based on laboratory tests:

$$G_{13} = \frac{E_1 E_3}{\left(1 + 2\nu_{13}\right) E_1 + E_3} \qquad (2)$$

The boundary conditions correspond to a null normal displacement on the vertical faces and the lower horizontal face. The upper horizontal face is loaded with stress components.

All simulations have been carried out following two principal phases:

➢ first phase corresponds to the calculation of the initial state of equilibrium before shaft sinking onset ;

➢ second phase corresponds to the shaft sinking simulation in 31 successive stages.

2.3 MODEL VALIDATION

The numerical model was validated based on 3 x 3 x 4 calculated stress profiles compared with the analytical solutions of the stress field in elastic homogeneous medium around an infinite cylindrical shaft. Error acceptance has been set as very low in order to minimize errors due only to numerical modelling artefacts in the overall procedure.

Table 2 recapitulates the maximum absolute and relative error (between numerical and analytical results) made near the various measurement points.

2.4 ANALYSIS OF THE MEASUREMENTS OBTAINED ON THE VARIOUS INSTRUMENTS OF THE VIRTUAL EXPERIMENTAL DEVICE

2.4.1 Measurements obtained in the canonical loading simulations

Measurements obtained correspond to the influence coefficients relating these measurements to the corresponding components of the initial stress tensor. Basic analysis of these measurements allows to evaluate amplitude versus time fonction of each sensor (maximum, signal to noise ratio, gradients, etc.). Then analysis of these data (of the 42 graphs like those presented on figure 4.), instrument by instrument, offers a unique mean to identify quantitatively numerous singular conditions as, for example:

➢ no measuring instrument considered individually shows a satisfactory sensitivity to the whole components of $[\sigma^0]$. This result is clearly accentuated by the 2D final geometry of the experiment, once the shaft has been completely passing by the monitored volume of rock;

➢ redundancy of sensors inside a same instrument (extensometer) can not be justified in terms of quantitative improvement of the overall instrumentation set up;

➢ a sensor may show a narrow predicted useful data range to be back analysed; this can be anticipated by further considerations on the front face working progress of the opening;

➢ best numerical conditioning is to be obtained by combining instruments bringing of additional information, for example CSIRO cells (information on all the components of $[\sigma^0]$ except σ^0_{ZZ}) and axial extensometer 3 (information only on σ^0_{ZZ}).

2.4.2 Numerical results of the shaft sinking

The graphs of evolution of the numerically simulated measurements obtained on each instrument in the triaxial case (loaded with an estimated stress state representative of the experiment depth) are presented on figure 4. On can note some of the relevant points below:

➤ the order of amplitude of the measurement variations obtained on CSIRO 1 cell (more than 4000 µm/m in extension) is relatively high taking into account the range of recommended use for CSIRO cells, i.e. 2500-3000 µm/m. This remark thus encourages to recommend the taking of this cell away the shaft side wall;

➤ the variations of maximum displacement obtained on the sensors of extensometers 1 and 2 lie between 500 and 2400 µm (4000 to 8500 µm for extensometer 3). These variations are at the same time sufficient with respect to the precision of these instruments ($\pm$ 50 µm) and remain quite lower than their measurement range (105 µm);

➤ the variations of displacement obtained on extensometer 3 are at the same time sufficient with respect to their precision ($\pm$ 50 µm) and lower the tolerance range considered for this instrument (100000 µm);

➤ the variations of measurements obtained by the inclinometer lie between 100 and 1000 µm. These variations are weak, but remain sufficient for the points closest to the shaft (points n°3 to 5). On the other hand, they become insufficient, with respect to the device precision ($\pm$ 100 µm/m) for the points furthest away from the shaft (points n°1 and 2);

➤ the comparison (figure 3) of the displacements obtained at the position of the reference points of extensometers 1, 2 and of the inclinometer with those obtained at the position of their first measurement point (point n°1) shows well that displacements of the reference positions are significant and do not have to be neglected.

Those simulations have been completed with elastoplastic modelling of the shaft sinking in order to finalize the layout of the experiment. As this article is focus on the under excavation method which requires elastic model, the result of elastoplastic are not shown here.

3. DATA INVERSION STRATEGY

3.1 PRESENTATION

 Increasing number of measurements of varied types make the data to be selected and to be inversed quite difficult. Because there are a too great number of possible choices which relate at the same time to:

➢   number of sensors (data sub sets) to be inversed;

➢   temporality of the considered measurement intervals compared to the face advance;

➢   number and width of measurement intervals;

➢   relative temporal shift between the considered intervals, etc…

At the same time, as it was mentioned for the under-excavation technique, by Wiles & Kaiser [15] who proposed a methodology of selection of the data to be taken into account in the inversion (figure 5). Wiles and Kaiser propose for the stage B three different strategies (figure 6):

➢   "simple interval" (SI);

➢   "multiple intervals with shifted origins" (MISO);

➢   "multiple intervals with common origins" (MICO).

In this study, we explored a large set of possible choices for combination of instruments at stage A (12 combinations of instruments: C1, C2, C3, C1-E3, C2-E3, C3-E3, C1-C2-C3, C1-C2-C3-E3, E1-E2-I1, E1-E2-I1-E3, C1-C2-C3-E1-E2-I1 and C1-C2-C3-E1-E2-I1-E3) and all possible combinations for stages B and C.

Moreover, for stage B, we tested a fourth procedure (called TOT), which consists in taking into account all the possible intervals of measurement in the inversion. The aim of this last approach is to be able to give a more complete answer on the influence of each assumption on the estimated initial stresses. It is thus possible to establish the type of instrument or the intervals of measurement which it is necessary to consider in the inversion to be able to limit to the maximum the influence of the assumptions that one wishes to test.

3.2 APPLICATION TO THE TRIAXIAL LOADING SIMULATION

The triaxial tests simulation allows to select the most favourable inversion methods. The application of the methodology of inversion led to 15660 inversions to be run through an automated function implemented in the interpretative tool (1305 by combination of instruments). All possible inversions are studied in order to have a better estimation of stresses and their linked error.

The assumptions used in this method being the same as those supposed to build the matrix [M], we have to find, after inversion, the initial stress tensor imposed on the model boundaries if the matrix [M] is well conditioned (the matrix conditioning is the ratio of its greater eigenvalue on its smaller eigenvalue). It is allowed that a conditioning ranging between 0 and 10 is "very good", "good" between 10 and 20, "acceptable" between 20 and 30, and that beyond 30, the inversion of measurements presents a significant amplification risk of numerical errors.

Figure 7 shows the cumulative distribution (P<(x), percentage of case where x is lower than a given value) of the conditioning value according to the combination of instruments taken into account in the inversion. The conditioning value of the influence matrix (figure 7) is very variable according to the combination of instruments considered in the inversion. Best conditioning is not obtained by considering all the instruments, but only the CSIRO cells and the extensometer located in the shaft axis (E3). For these two combinations of instruments, almost all the inversion methods lead to an acceptable conditioning (< 30). On the other hand, the inversions only carried out on the extensometers except the one placed axially inside the front face of the shaft and inclinometer (E1-E2-I1) never lead to an acceptable conditioning.

Figure 8 shows the distribution of the maximum relative difference (noted DEVMAX) between the values of stresses imposed on the model $\sigma_i^{0\,imp}$ and those estimated by inversion of numerically simulated measurements $\sigma_i^{0\,est}$ (normalization with the average stress):

$$DEVMAX = \max_{i=XX,YY,ZZ,YZ,XZ,XY} \left(\frac{\left| \sigma_i^{0\,est} - \sigma_i^{0\,imp} \right|}{\left(\sigma_1^{0\,imp} + \sigma_2^{0\,imp} + \sigma_3^{0\,imp} \right)/3} \right) \tag{3}$$

As for conditioning, we note that the difference between the back calculated and prescribed stresses is very variable according to the combination of instruments considered in the inversion. The combinations of instruments giving place to a bad conditioning tend overall to generate a more important error on the estimated stresses. This global correlation between the conditioning (COND) of the influence matrix and the made error DEVMAX on the estimated stresses is shown on figure 9.

However, one can note certain differences between figures 7 and 8. For example, the combination of instruments giving place to best conditioning (C1-C2-C3-E3) is not that which produces less error on the estimated stresses (even if it remains among the best).

A limited number of inversion cases were selected. These favourable inversion cases are those which lead at the same time to best conditioning and the weakest error on the prescribed stresses (COND < 30, DEVMAX < 1%). The number of cases thus selected for the study continuation is 2151, that is to say 13.7 % of the number of initial inversions.

Figure 10 shows the distribution of the favourable inversion cases according to the combination of instruments chosen in inversion. This one revealed the following points:

➢ the most favourable inversion conditions are those which consider only measurements of CSIRO 1cell and extensometer 3;

➢ no inversion taking into account only measurements of the extensometers out of shaft and the inclinometer leads to favourable inversion conditions. It is the same for all the inversions including only the C3 cell;

➢ CSIRO cells leading to the best inversion conditions are, in the order, the C1, C2 and C3 cell. We respectively notice that this gradation is correlated with the distance from these cells compared to the shaft, those being of 1.85 m, 3.90 m and 4.81 m ;

➢ the advantage of extensometer 3, from the point of view of the inversion quality improvement, appears clearly on figure 10 (compare two by two results obtained without the extensometer 3 and those obtained with the same instruments, plus extensometer 3).

4. CONCLUSION

Within the framework of REP experiment in Bure (France), Andra and INERIS intend to develop an under-excavation interpretative technique in order to reduce uncertainty on the in-situ stress state in the Callovo-Oxfordian argillite formation.

A 3D synthetic numerical study has then been completed in order to assess quantitatively the overall reliability and performance of the under-excavation technique. The methodology has been extended in the way that:

- intermediate results needed as calculated influence coefficients and total predicted measurements of all varied sensors to be implemented could be back analysed in terms of operational recommendations, regarding a given sensor or a subset of sensors;

- inversion numerical strategies are explored based on calculated indicators able to quantify comparatively different instrumentation schemes versus excavation front face overall lay outs, aiming to minimize computational undesired artefacts.

This study is one of the studies necessary to the REP experiment design, nevertheless, the calculations presented in this article allow to improve the experimental device by:

- moving away CSIRO 1 from the shaft side wall of approximately 3 m;

- relocating the inclinometer sensors by reducing the bars length and by increasing the number of measurement points.

Moreover, this study shows that the reference points of the extensometers out of shaft and the inclinometer will move significantly in the shaft passage (comparison of figure 3a with figure 3b). This problem can be avoided by not inversing measurements out of shaft that starting from the stage – 460 m.

3D numerical conception of an under-excavation interpretative experiment, e.g. aiming to back estimate an unique, overall quantitative result as field stresses, appears to be of major interest for optimizing data quality to be recorded, first for a specific sensor considered, secondly and moreover for the quality of the overall instrumentation scheme, or whatever can be called "information wealth" of data set to be recorded. This "optimal 3D design" approach includes complex factors usually difficult to handle at the same time for the rock mechanics engineer as:

1- best instrumentation coverage of the 3D complex geometry of the advancing excavation inside the instrumented volume of rock;

2- geomechanical properties of host rock to be monitored;

3- correct spreading of the varied instruments to be set up.

5. REFERENCES

[1] Collectif, 2001." Référentiel Géologique du site de Meuse/Haute-Marne – Tome 4 Le Callovo-Oxfordien », identification A RP ADS 99-005.

[2] Amadei, B., 1996. Importance of Anisotropy When Estimating and Measuring *In Situ* stresses in ROCK*, Int. J. Rock Mech. Min. Sci. & Geomech. Abstr.* Vol. 33, n°3, pp. 293-325.

[3] Bigarré, P., 1996. Casamance, Mesures de déformations, interprétation des données, rapport INERIS SSE/PBi/DMi/96-26EB51/RN01 (réf. ANDRA : B RP 1.INE 96.009). Technical Note

[4] Bigarré, P., 1998. Mt. Terri Project, Phase III, Stress Measurement Experiment, rapport INERIS SSE-98-26EF10/RN01. Technical report.

[5] Galybin, A.N., Dyskin, A.V. & Jewell R.J., 1997. A measuring scheme for determining in situ stresses and moduli at large scale. *Int. J. Rock Mech. Min. Sci.*, Vol. 34, n° 1, pp. 157-162. Technical note.

[6] Lahaie, F. & Renaud, V., 2004. Etude de sensibilité de la technique de sous-carottage - Rapport final, Accord technique ANDRA-INERIS, Mesures de contraintes et déformations, Lot A.1.2.3, rapport INERIS DRS-04-37797/RN13 (réf. ANDRA : D RP 1INE-04-001/A). Technical report.

[7] Lekhnitskii, S. G., 1981. *Theory of elasticity of an anisotropic elastic body*, MIR, Moscow.

[8] Martin, C. D., Kaiser, P. K. & Christiansson, R., 2003. Stress, instability and design of underground excavations. *Int. J. Rock Mech. Min. Sci.*, Vol. 40, n° 7-8, pp. 1027-1047.

[9] Martin, C.D. / Lanyon, G.W., 2003. Measurement of in-situ stress in weak rocks at Mont Terri Rock Laboratory, Switzerland. *Int. J. Rock Mech. Min. Sci.*, Vol. 40, n° 7-8, pp. 1077-1088.

[10] Read, R.S., Martin, C.D., 1996. Technical summary of AECL's Mine-by Experiment Phase 1: Excavation response. AECL Report AECL-11311, Atomic Energy of Canada Limited.

[11] Souley, M., Su, K., Ghoreychi, M. & Armand, G., 2003. Constitutive models for rock mass numerical implementation, verification and validation. Brummer et al. (eds), © 2003 Swets & Zeitlinger B.V., Lisse, The Netherlands, ISBN 90 5809 581 9.

[12] Thompson, P.M. & Chandler, N.A., 2004. In situ rock stress determinations in deep boreholes at the Underground Research Laboratory. *Int. J. Rock Mech. Min. Sci.* Vol. 41, n° 8, pp. 1305-1316.

[13] Tonon, F. & Amadei, B., 2003. Stresses in anisotropic rock masses: an engineering perspective building on geological knowledge. *Int. J. Rock Mech. Min. Sci.*, Vol. 40, n° 7-8, pp. 1099-1120.

[14] Wiles, T. D. & Kaiser, P. K., 1994. *In Situ* Stress Determination Using the Under-excavation Technique – I. Theory. *Int. J. Rock Mech. Min. Sci. & Geomech. Abstr*. Vol. 31, n° 5, pp. 439-446

[15] Wiles, T. D. & Kaiser, P. K., 1994. *In Situ* Stress Determination Using the Under-excavation Technique – II. Applications. *Int. J. Rock Mech. Min. Sci. & Geomech. Abstr*. Vol. 31, n° 5, pp. 447-456

Parameter	Facies A	Facies B & C
Wet density	$\rho_h = 2420$ kg/m^3	
Young modulus $\perp$ to the plan of transverse isotropy	$E_3 = 5200$ MPa	$E_3 = 5200$ MPa
Young modulus // to the plan of transverse isotropy	$E_1 = 6300$ MPa	$E_1 = 6300$ MPa
Poisson's ratio	$\nu_{12} = \nu_{13} = 0{,}30$	
Shear modulus G_{13}	$G_{13} = 2144$ MPa	$G_{13} = 2144$ MPa

Table 1: Mechanical characteristics of facies A, B and C

	σ_{rr}	$\sigma_{\theta\theta}$	σ_{zz}	$\sigma_{r\theta}$
Relative error	1.58%	1.01%	1.21%	0.62%
Absolute error (MPa)	6.71E-02	1.00E-03	1.00E-03	2.13E-03

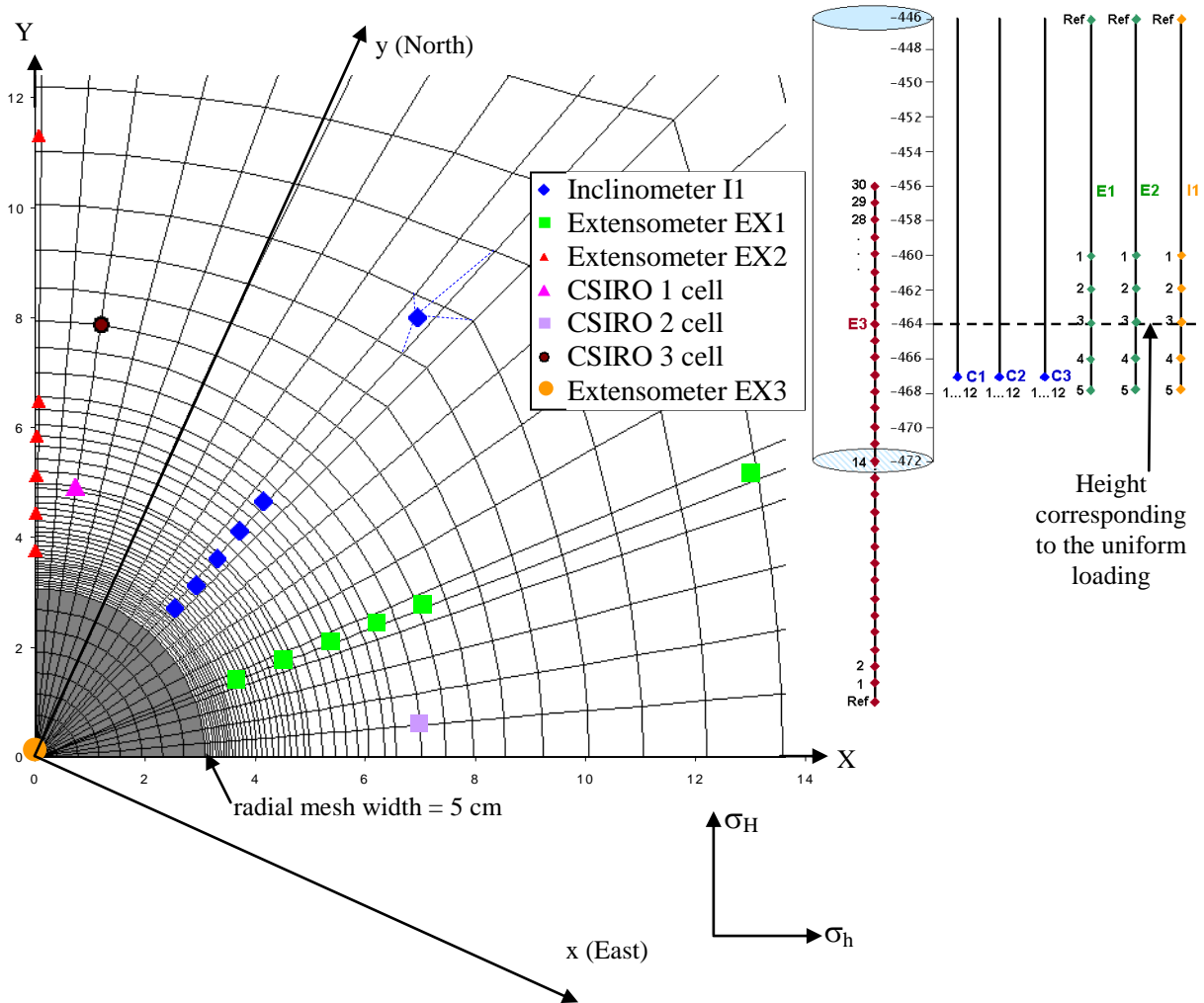*Table 2: Absolute and relative maximum errors between numerical and analytical results*

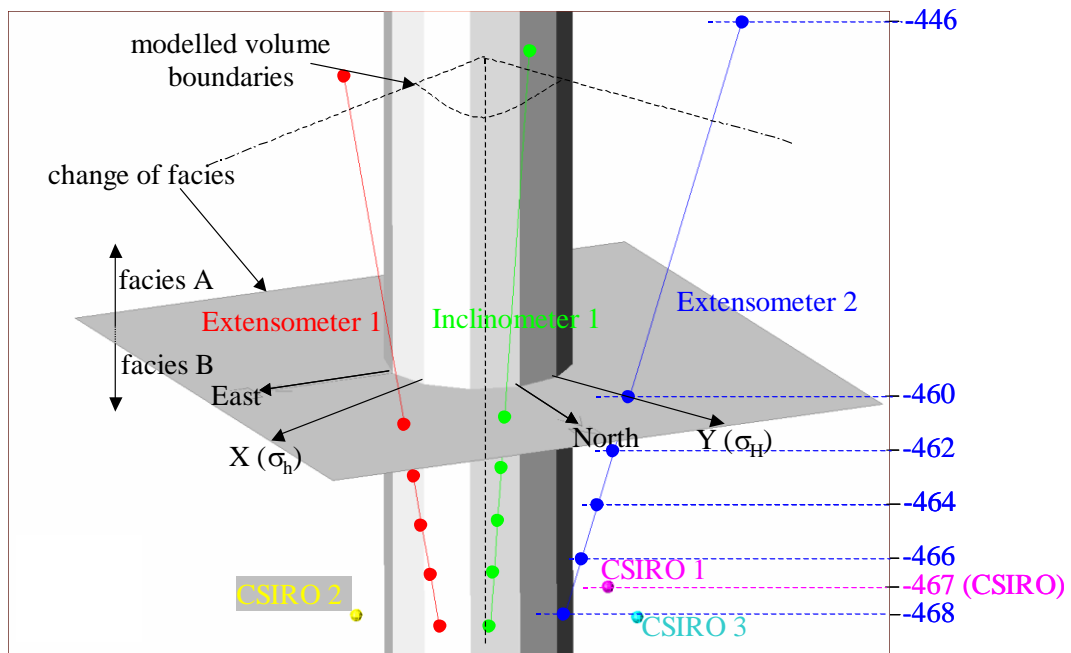*Figure 1 : Detail of the horizontal meshing and localisation of measurement points*

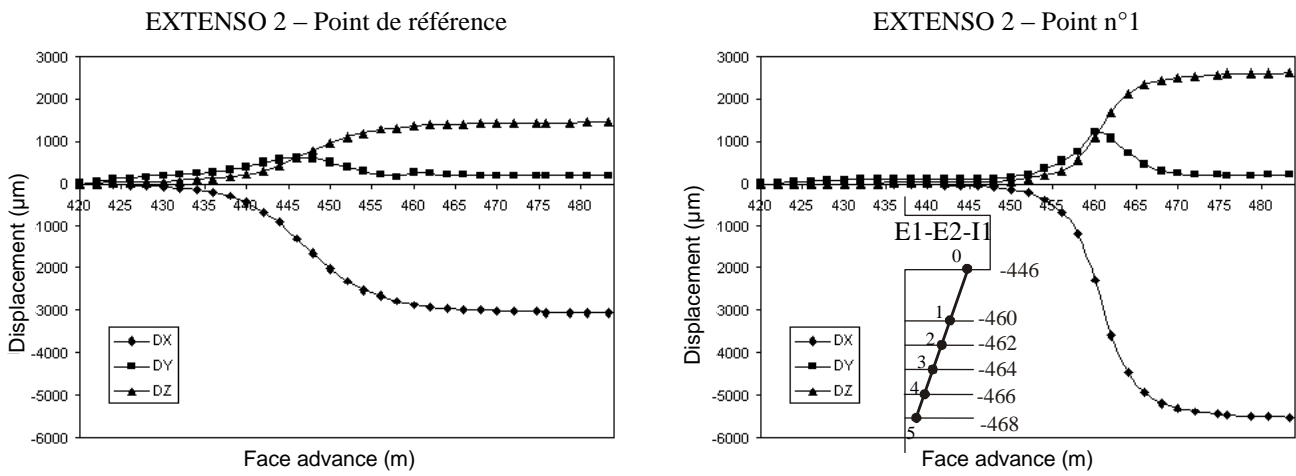*Figure 2 : 3D overview of the measurement device around the shaft*

Figure 3 : Comparison between displacements of the n°1measurement and reference points of extensometer 2
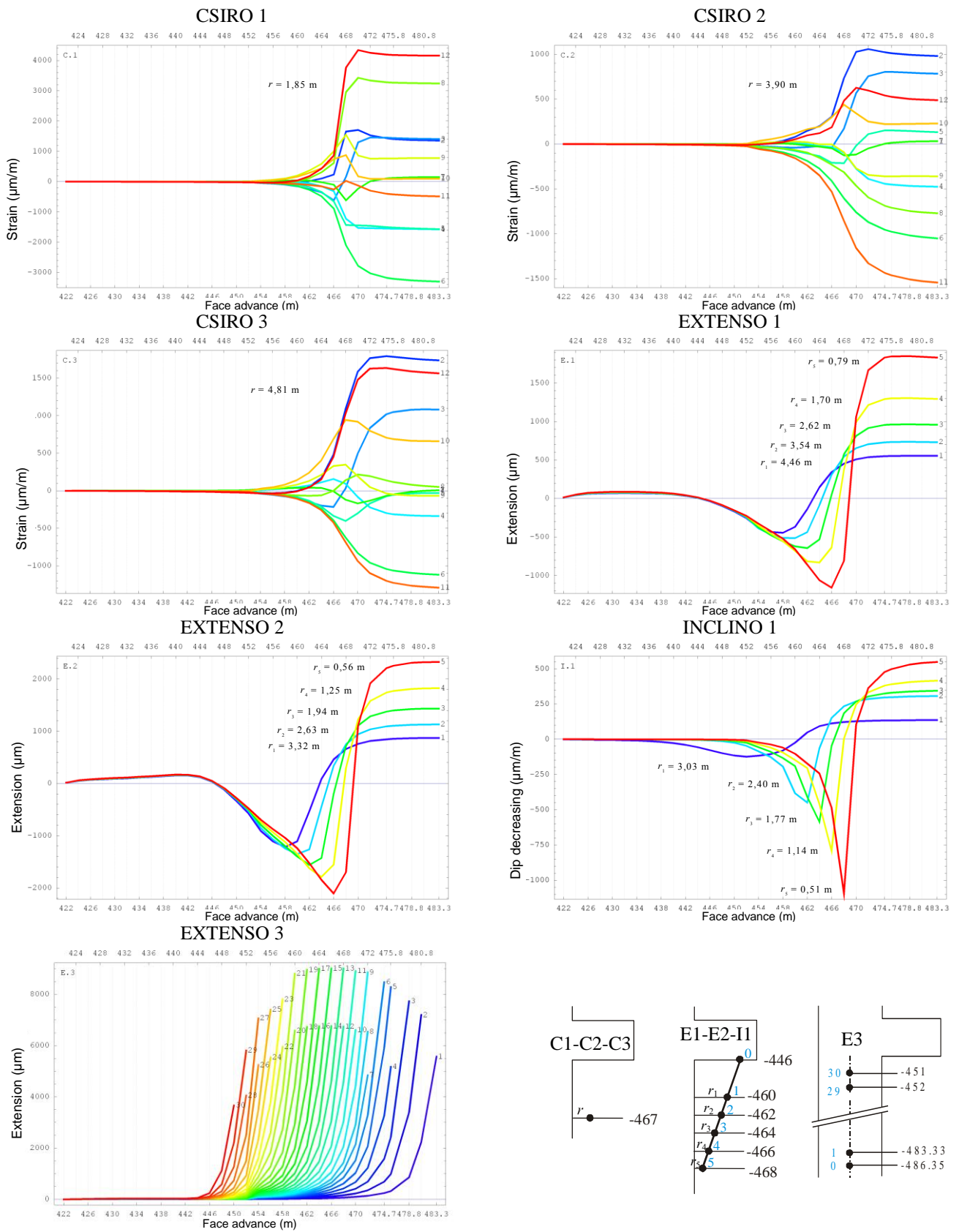
Figure 4 : Typical measurements provided by the various sensors of the modelled device
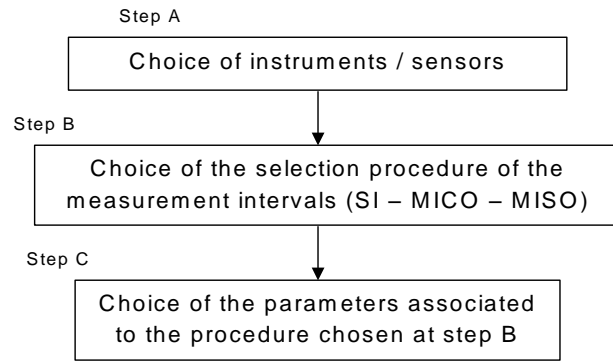
Step A

Choice of instruments / sensors

Step B

Choice of the selection procedure of the
measurement intervals (SI – MICO – MISO)

Step C

Choice of the parameters associated
to the procedure chosen at step B

*Figure 5 : Selection methodology of the data to be taken into account in the inversion
(according to Wiles & Kaiser [15])*

(a) Single-interval (SI)

$d=3$ — d: interval width

i_0 i i_{max}

(b) Multiple-intervals with shifted origins (MISO)

$a=4$ — a: interval number

$d=3$

i_0 $i \longrightarrow t=2$ i_{max}

(c) Multiple-intervals with common origins (MICO)

$a=4$

i_0 $i \longrightarrow t=2$ — t: position increment between 2 successive intervals i_{max}

(d) Total (TOT)

$a=a_{max}$

i_0 $i \longrightarrow t=1$ progress steps are indexed $\longrightarrow i_{max}$
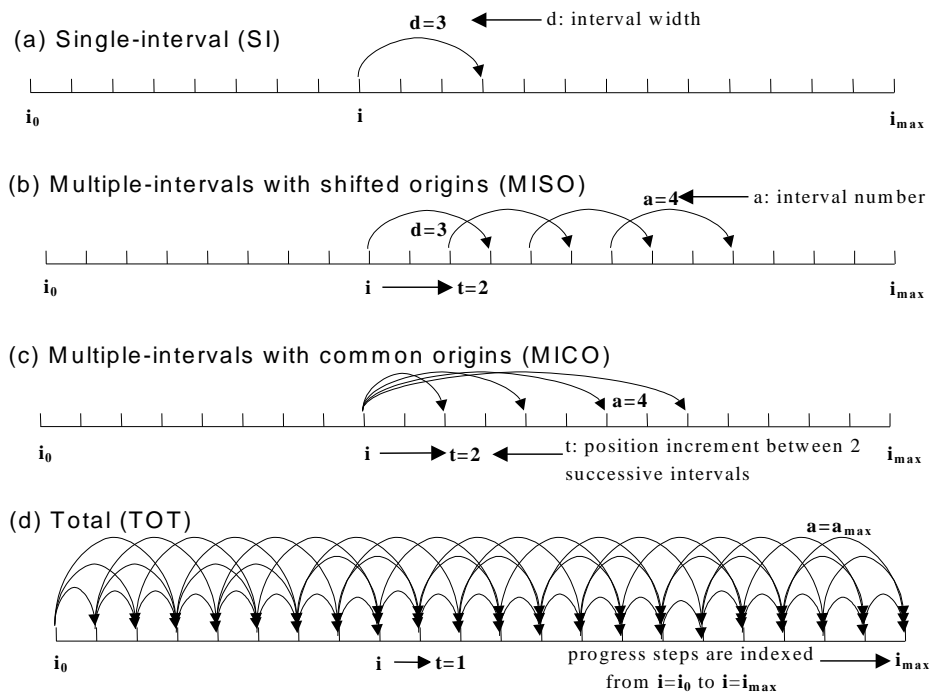from $i=i_0$ to $i=i_{max}$

*Figure 6 : Selection procedures of intervals of measurements taken into account in the
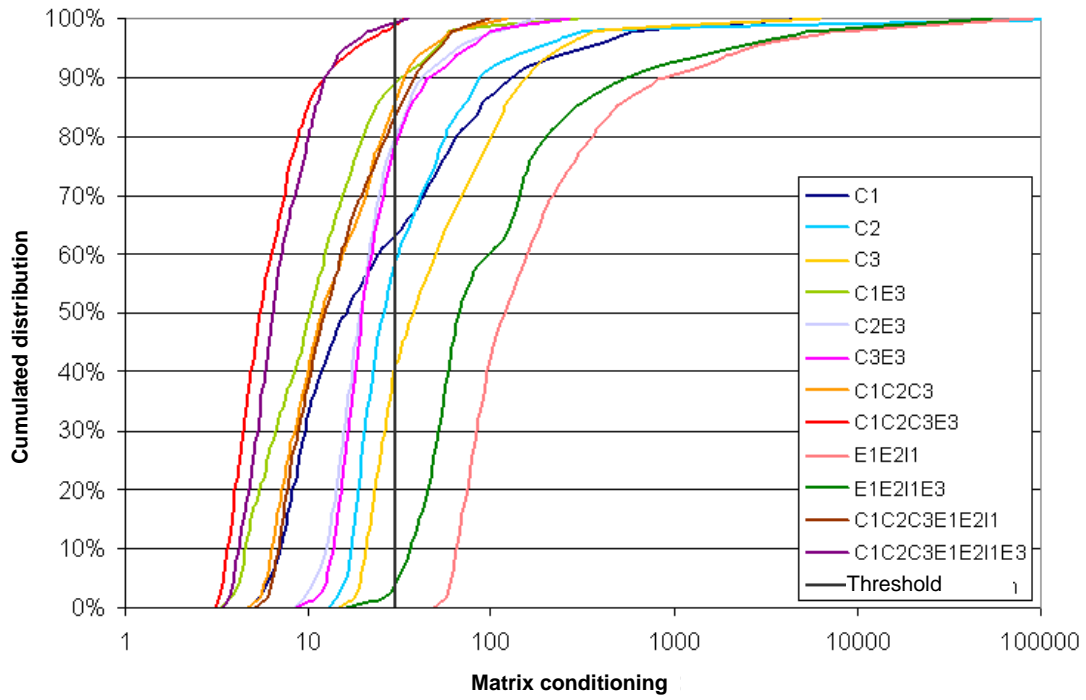inversion = stage B (adapted of Wiles & Kaiser [15])*

Figure 7 : Cumulative distribution of the influence matrix conditioning according to the combination of instruments considered in the inversion
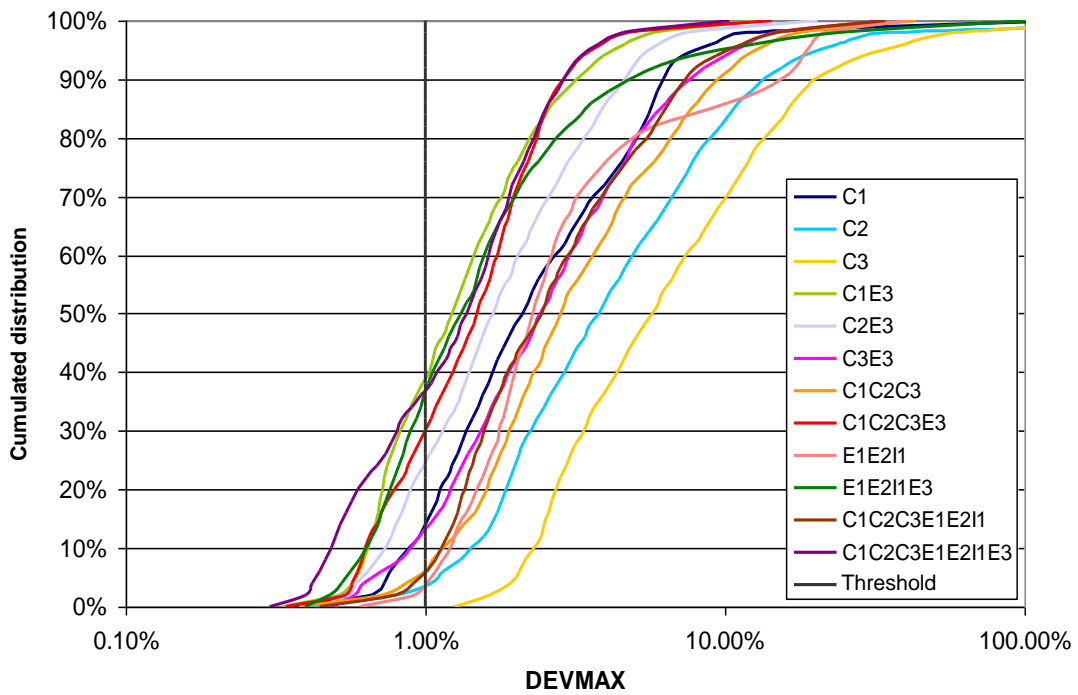

Figure 8 : Distribution of the maximum relative difference (DEVMAX) between the estimated stresses and the prescribed stresses in the triaxial case
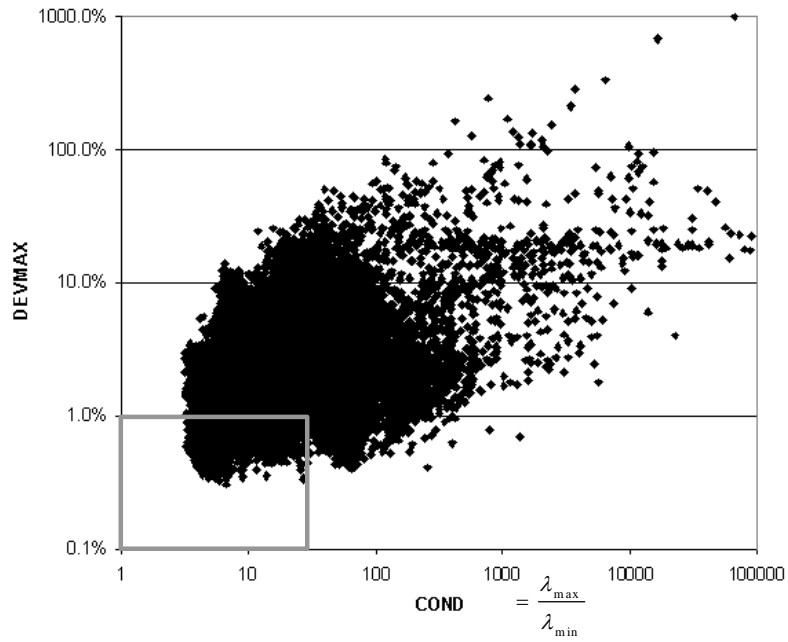
Figure 9 : Error made on the prescribed initial stresses according to influence matrix conditioning
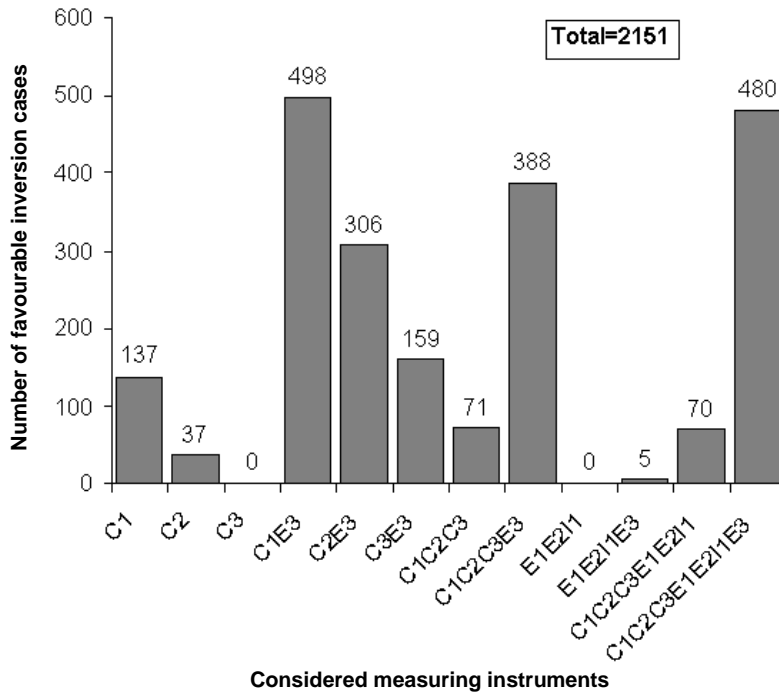

Figure 10 : Importance of the choice of the instruments in obtaining favourable inversion conditions